10

Carbon Nanotube Y-Junctions

Prabhakar R. Bandaru
University of California, San Diego

10.1 Introduction

In recent years, carbon nanotubes (CNTs) have emerged as one of the foremost manifestations of nanotechnology and extensive research has been expended in probing their various properties. While many desirable attributes in terms of electrical, mechanical, and biological properties have been attributed to CNTs, many obstacles remain before their widespread, practical application (Baughman et al. 2002) becomes feasible. Some of the foremost hindrances are (1) the variation of properties from one nanotube to another, partly due to the unpredictability in synthesis and the random occurrence of defects and (2) the lack of a tangible method for wide-scale synthesis. Generally, the variation of properties is a natural consequence of nanoscale structures and could be difficult to solve, at least in the short term. It would then seem that fundamentally new ideas might be needed. Some interesting viewpoints are also being considered, where defect manipulation could be used on purpose (Nichols et al. 2007). Wide-scale synthesis methods, for example, by aligning the nanotubes with the underlying crystal orientation (Kang et al. 2007) have recently proved successful, but it is still not clear as to whether such methods would allow for practical implementation, say on the scale of silicon microelectronics.

In this context, it would be pertinent to pause and consider the rationale for the use of nanotubes, especially in the context of electronic characteristics and devices. Carbon-based nanoelectronics technologies (McEuen 1998) promises greater flexibility compared to conventional silicon electronics, one example being the extraordinarily large variety of carbon-based organic structures. It would then be interesting to look into the possible implications of this "large variety," particularly with respect to the morphology and its associated properties. Such an outlook gives rise to the possibility of examining nonlinear forms, some examples of which are depicted in Figure 10.1. While Y-junctions can be used as three-terminal switching devices or diodes, helical nanostructures can give rise to nanoscale inductors or, more interestingly, a sequence of metallic and semiconducting junctions (Castrucci et al. 2004). It is to be noted at the outset that we now seek to explore completely novel forms of electronics as laid out, for example in the International Technology Roadmap for Semiconductors (ITRS) recommendations on *Emerging Research Devices*. We quote "The dimensional scaling of CMOS devices and process technology, as it is known today, will become much more difficult as the industry approaches 16 nm (6 nm physical channel length) around the year 2019 and will eventually approach an asymptotic end. Beyond this period of traditional CMOS scaling, it may be possible to continue functional scaling by integrating alternative electronic devices onto a silicon platform. These alternative electronic devices include 1D structures such as *CNTs*…." The purpose of investigating novel nanotube morphologies is to demonstrate many of the "compelling attributes" as laid out in the ITRS roadmap, which include (1) "room temperature operation," (2) "functionally scalable by orders of magnitude," and (3) "energy dissipation per functional operation substantially less than CMOS." We will show specifically how the exploration of Y-junction topologies would help in laying the foundation for an entirely new class of electronic and optical devices.

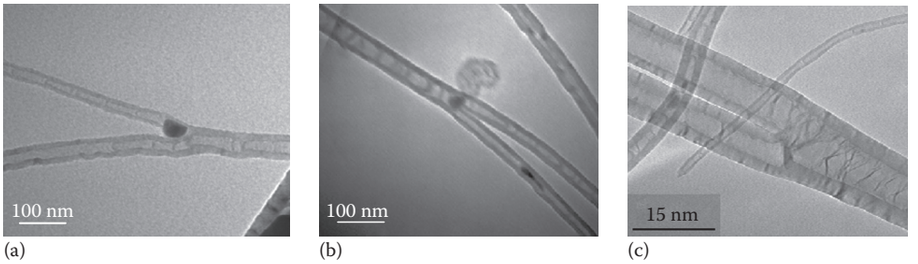

FIGURE 10.1 The nano-engineering of carbon nanotubes (CNTs) to produce nonlinear structures is manifested most clearly through the Y-junction morphology. Such structures can be prepared by adding carbide forming elements, such as Ti, Zr, and Hf to ferrocene based thermal CVD, at different branching angles [i.e., (a) vs. (b)] and spatial locations of catalyst particles [i.e., (a) vs. (c)] through varying the growth conditions.

10.1.1 Carbon Nanotubes

We commence with an overview of the underlying constituents of Y-shaped structures—linear nanotubes. Several comprehensive expositions (Dai 2002) of the fundamental aspects are extant in literature (Ajayan 1999, Dai 2002, McEuen et al. 2002, Dresselhaus et al. 2004, Bandaru 2007). Nanotubes are essentially graphene sheets rolled up into varying diameters (Saito et al. 1998) and are attractive from both a scientific and a technological perspective, as they are extremely robust (Young modulus approaching 1 TPa) and, at least in pristine forms, chemically inert. By varying the nature of wrapping of a planar graphene sheet and consequently their diameter, nanotubes can be constructed to be either semiconductors or metals (Yao et al. 1999), which can be used in electronics (Collins and Avouris 2000). In the literature, there are a variety of tubular structures composed of carbon that are referred to as nanotubes (single-walled nanotubes [SWNTs] and multi-walled nanotubes [MWNTs]) when the graphene walls are parallel to the axis of the tube, and as nanofibers for other configurations, e.g., where the graphene sheets are at an angle to the tube axis.

The electrical and thermal conductivity (Hone et al. 2000) properties of both SWNTs (Tans et al. 1997) and MWNTs have been well explored. While SWNTs (diameter ~1 nm) can be described as quantum wires due to the ballistic nature of electron transport (White and Todorov 1998), the transport in MWNTs (with a diameter in the range 10–100 nm) is found to be diffusive/quasi-ballistic (Delaney et al. 1999, Buitelaar et al. 2002). Quantum dots can be formed in both SWNTs (Bockrath et al. 1997) and MWNTs (Buitelaar et al. 2002) and the Coulomb blockade and the quantization of the electron states can be used to fabricate single-electron transistors (Tans et al. 1998). Several electronic components, based on CNTs, such as single-electron transistors (SETs) (Tans et al. 1998, Freitag et al. 2001, Postma et al. 2001), nonvolatile random-access memory (RAM) (Rueckes et al. 2000, Radosavljevic et al. 2002), field-effect transistors (FET) (Radosavljevic et al. 2002), and logic circuits (Bachtold et al. 2001, Martel et al. 2002, Javey et al. 2003), have also been fabricated. However, most of these devices use conventional lithography schemes and electronics principles, either using nanotubes as conducting wires or modifying them along their length, say through atomic force microscopy (AFM)-based techniques (Postma et al. 2001). While extremely important in elucidating fundamental properties, the above experiments have used external electrodes, made through conventional lithographic processes, to contact the nanotubes and do not represent truly nanoelectronic circuits. Additionally, the well-known metal oxide semiconductor field-effect transistor (MOSFET) architecture is used, where the nanotube serves as the channel between the electrodes (source and drain), and a SiO_2/Si-based gate modulates the channel conductance. In other demonstrations, cumbersome AFM manipulations (Postma et al. 2001) may be needed.

It would, therefore, be more attractive to propose new nanoelectronic elements to harness new functionalities peculiar to novel CNT forms such as nanotubes with bends, Y-junctions (Bandaru et al. 2005), etc. One can also envision a more ambitious scheme and circuit topology where both interconnect and circuit elements are all based on nanotubes, realizing true nanoelectronics (Figure 10.2). For example, the nanotube-based interconnect does not suffer from the problems of electro-migration that plague copper-based lines, due to the strong carbon–carbon bonds, and can support higher current densities (Collins et al. 2001b) (~10 μA/nm^2 or 10^9 A/cm^2 vs. 10 nA/nm^2 or 10^6 A/cm^2 for noble metals such as Ag). Additionally, the predicted large thermal conductivity (Kim et al. 2001) (~3000 W/mK at 300 K), up to an order of a magnitude higher than copper, could help alleviate the problem of heat dissipation in ever-shrinking devices. Developing nanotube-based devices, besides miniaturization and lower power consumption, could also allow us to exploit the advantages of inherently quantum mechanical systems for practical devices, such as ballistic transport and low switching voltages (Wesstrom 1999) (~26 mV at room temperature $\equiv k_B T/e$).

10.1.2 Branched Carbon Nanostructures—Initial Work

At the very outset, any deviation from linearity, say in a branched Y-junction, must be accompanied by the disruption of the regular hexagonal motif. This can be accomplished, in the simplest case, by the introduction of pentagons and heptagons to account for the curvature (Iijima et al. 1992) (Figure 10.3a). Since the charge

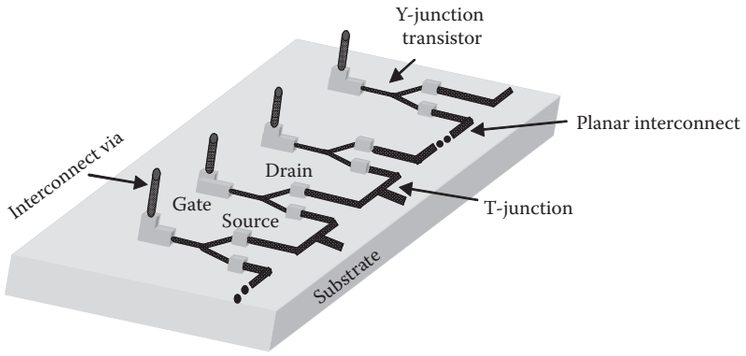

FIGURE 10.2 A conceptual view of a possible CNT technology platform, including Y-junction devices, interconnect vias and directed nanotube growth. The overall objective is to create nano devices with novel functionalities that go beyond existing technologies.

distribution is likely to be nonuniform in these regions, the interesting possibility of localized scattering centers can be introduced. For example, rectification behavior was posited due to different work functions of contacts with respect to metal (M) and semiconductor (S) nanotubes (electrostatic doping) on either side of the bend (Yao et al. 1999). Later in this chapter, we will discuss how this can be exploited for more interesting device electronics.

Nanotube junctions were formed through the use of high-energy (1.25 MeV) electron beam exposure (in a transmission electron microscope) based welding of linear SWNTs, at high temperature (800°C) welds SWNTs to form X-, Y-, or T-junctions was illustrated in Figure 10.3b and c (Terrones et al. 2002). The underlying mechanism invoked was primarily the "knock-off" of carbon atoms and *in situ* annealing. Molecular dynamics simulations intimate that vacancies and interstitials play a role. However, the purposeful synthesis of branched morphologies can be accomplished through chemical vapor deposition (CVD) methods. Preliminary work on individual Y-junctions, grown through CVD, in branched nano-channel alumina templates (Li et al. 2001) resulted in the observation of nonlinear *I–V* characteristics at room temperature through Ohmic contact (Papadapoulos et al. 2000) and tunneling conductance (Satishkumar et al. 2000) measurements. From an innate synthesis point of view, nanotubes with T-, Y-, L-junctions, and more complex junctions (resembling those in Figure 10.1), were initially observed in arc-discharge produced nanotubes (Zhou and Seraphin 1995). Beginning in 2000, there was a spate of publications reporting on the synthesis of Y-junctions through the use of organometallic precursors, such as nickelocene and thiophene, in CVD (Papadapoulos et al. 2000, Satishkumar et al. 2000). Y-junction (Li et al. 2001) and multi-junction carbon nanotube networks (Ting and Chang 2002) were also synthesized through the pyrolysis of methane over cocatalysts and through the growth on roughened Si substrates. However, the mechanism of growth was not probed into adequately.

AQ1

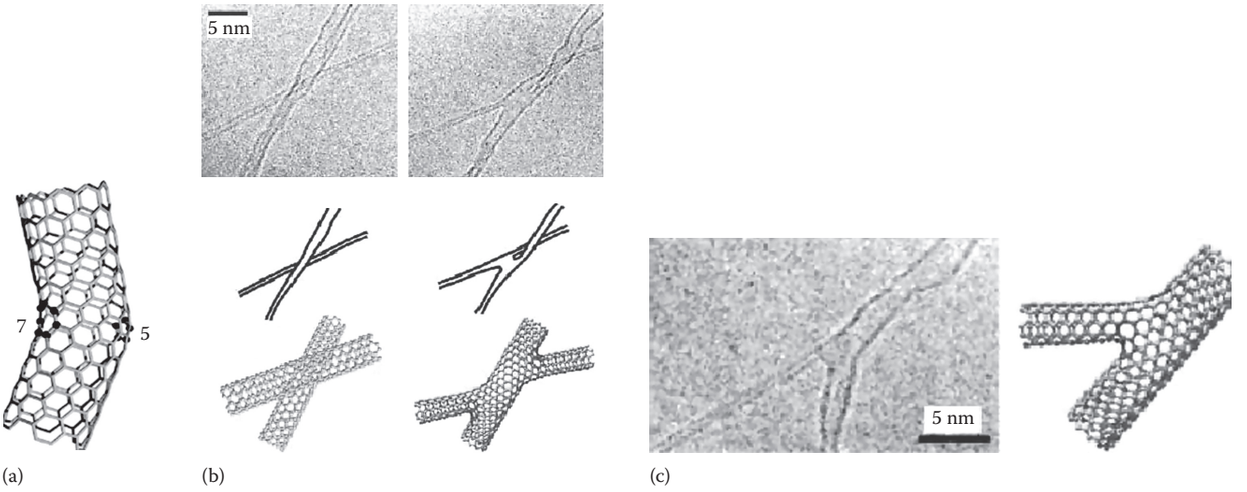

FIGURE 10.3 (a) A bend in a nanotube, say in a Y-junction, introduces regions of positive and negative curvature. The associated heptagons and pentagons can have local excess/deficit of charge and can be used as scattering centers for nanoelectronics. (From Yao, Z. et al., *Nature*, 402, 273, 1999. With permission.) (b) X-shaped and (c) Y-shaped nanotube molecular junctions can be fabricated by irradiating crossed single walled nanotube junctions with high energy (~1.25 MeV) and beam intensity (10 A/cm^2) electron beams. (From Terrones, M. et al., *Phys. Rev. Lett*., 89, 075505, 2002. With permission.)

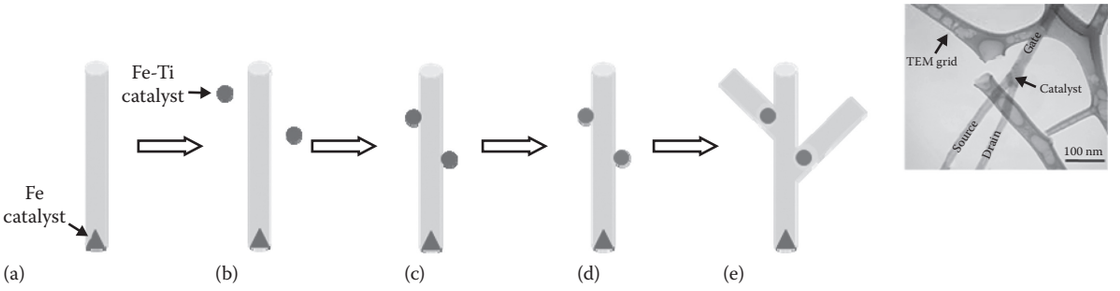

FIGURE 10.4 The postulated growth sequence of a Y-junction nanotube (Gothard et al. 2004) involves: (a) Initial seeding of a straight nanotube through conventional catalytic synthesis (Teo et al. 2004), (b) Ti-doped Fe catalyst particles (from ferrocene and $C_{10}H_{10}N_4Ti$) attach (c) to the sidewalls and nucleate (d) the side branches (e).

10.2 Controlled Carbon Nanotube Y-Junction Synthesis

It is to be noted at the very outset that the Y-junctions synthesized are quite different in form and structure compared to crossed nanotube junctions (Fuhrer et al. 2000, Terrones et al. 2002), where the nanotubes are individually placed and the junctions are produced through electron irradiation (Terrones et al. 2002). Significant control in the growth of Y-junction nanotubes (Gothard et al. 2004) on bare quartz or SiO_2/Si substrates through thermal CVD was accomplished through the addition of Ti-containing precursor gases to the usual nanotube growth mixture. In one instance, a mixture of ferrocene ($C_{10}H_{10}Fe$), xylene ($C_{10}H_{10}$), and a Ti-containing precursor gas-$C_{10}H_{10}N_4Ti$ was decomposed at 750°C in the presence of flowing argon (~600 sccm) and hydrogen (75 sccm) carrier gases. The two-stage CVD reactor consisted of (1) a low temperature (~200°C) preheating chamber for the liquid mixture vaporization followed by (2) a high temperature (~750°C) main reactor. A yield of 90% MWNT Y-junction nanotubes, which grew spontaneously on quartz substrates in the main reactor, was obtained. The mechanism for the Y-junction growth was hypothesized to depend on the carbide-forming ability of Ti as measured by its large heat of formation (ΔH_f of –22 Kcal/g-atom). The Ti-containing Fe catalyst particles seed nanotube nucleation by a *root growth* method, in which carbon was absorbed at the root and then ejected to form vertically aligned MWNTs (Figure 10.4a). As the supply of Ti-containing Fe catalyst particles continues (Figure 10.4b), some of the particles (Fe-Ti) attach onto the sidewalls of the growing nanotubes (Figure 10.4c). The catalysts on the side then promote the growth of a side branch (Figure 10.4d), which when further enhanced forms a full-fledged Y-junction. The correlation of the carbide-forming ability to branch formation was also supported by Y-junction synthesis in Hf-, Zr-, and Mo-doped (Choi and Choi 2005) Fe catalyst particles (Gothard et al. 2004), which also have large ΔH_f (HfC: –26 Kcal/g-atom and ZrC: –23 Kcal/g-atom). It was generally found that the use of Zr and Hf catalysts yields larger diameter Y-junctions.

The ratio of the Ti-precursor gas and the feedstock gases could be adjusted to determine the growth of the side-branches at specific positions (Figure 10.5). For example, a decreased flow of the xylene gas, at a point in time, would halt the growth of the nanotube, while preponderance of the Fe-Ti precursor gas/catalyst particles would nucleate the branch. The Y-junction formation has also been found to be sensitive to temperature, time, and catalyst concentration. The optimal temperature range is

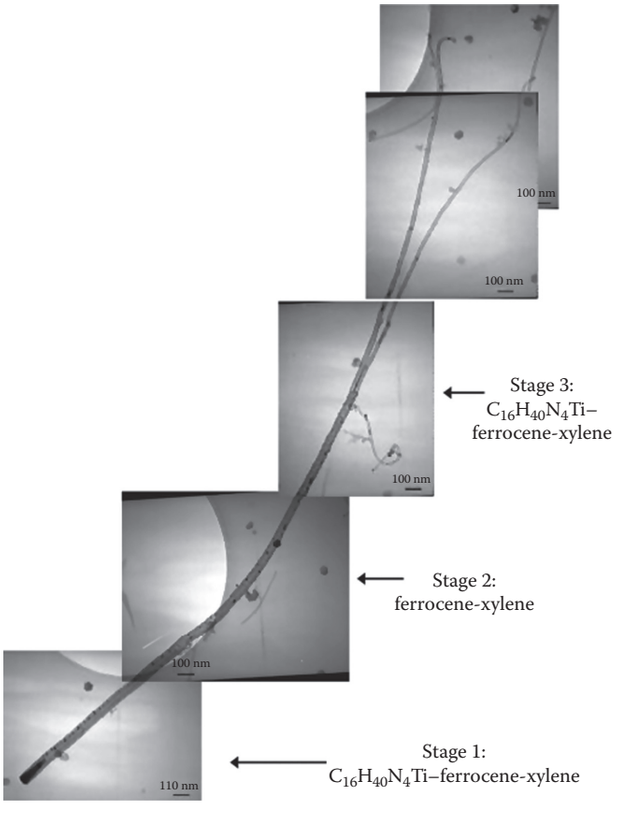

FIGURE 10.5 Controlled addition of Ti (see Stage 3) can induce branching in linear nanotubes. (From Gothard, N. et al., *Nano Lett.*, 4, 213, 2004. With permission.)

between 750°C and 850°C; below 750°C, the yield is very low and temperatures greater than 850°C produce V-shaped nanotube junctions. Y-junction CNTs with minimal defects, at the junction region, were obtained when the atomic compositions of Fe:Ti:C were in the ratio of 1:3:96.

The growth of the Y-junctions essentially seems to be a non-equilibrium phenomenon and various other methods have been found to be successful in proliferating branches, such as the sudden reduction of temperature during a normal tip growth process (Teo et al. 2004), where over-saturation by the carbon feedstock gas causes a surface-energy driven splitting of the catalyst particle and branch nucleation. Other catalyst particles, such as Ca and Si, have also been found to nucleate side branches (Li et al. 2001). The location of the junction is in any case a point of structural variation (Ting and Chang 2002), the control of which seems to determine the formation of Y-junctions and its subsequent properties. It should also be possible to undertake a rigorous thermodynamic analysis (Bandaru et al. 2007) to rationalize the growth of nonlinear forms.

10.3 Electrical Characterization of Y-Junction Morphologies

The initial research has focused mainly on the electrical characterization of the nanostructures. In a large part, it was motivated by the possible influence of topology on electrical transport, and supported through theoretical predictions of SWNT junctions. Current theoretical explanations of electrical behavior in Y-junctions are mainly based on SWNT Y-junctions, and the experimental demonstrations detailed in this chapter were made on both SWNT and MWNT Y-junctions (Papadapoulos et al. 2000, Satishkumar et al. 2000). It is speculated that relatively low temperature CVD methods that have been used to date may not be adequate to reliably produce SWNT-based Y-junctions with larger energetics (Terrones et al. 2002).

While SWNTs have been extensively studied theoretically (Ajayan 1999, Dai 2001), MWNTs have been relatively less scrutinized. An extensive characterization of their properties is found in literature (Forro and Schonenberger 2001, Bandaru 2007). MWNTs are generally found to be metal-like (Forro and Schonenberger 2001) with possibly different chiralities for the constituent nanotubes. Currently, there is some understanding of transport in *straight* MWNTs, where it has been shown that electronic conduction mostly occurs through the outermost wall, (Bachtold et al. 1999) and inter-layer charge transport in the MWNT is dominated by thermally excited carriers (Tsukagoshi et al. 2004). While the outer wall dominates in the low-bias regime (<50 mV), at a higher bias, many shells can contribute to the conductance with an average current carrying capacity of 12 μA/shell at room temperature (Collins et al. 2001b). In contrast to SWNTs with μm coherence lengths, the transport in MWNTs is quasi-ballistic (Buitelaar et al. 2002) with mean free paths <100 nm. Based on the above survey of properties in *straight* MWNTs, we could extend the hypothesis in that non-coherent electronic transport dominates the Y-junctions and other branched morphologies.

10.4 Carrier Transport in Y-Junction–Electron Momentum Engineering

The progenitor of a Y-junction topology, for electronic applications, was basically derived from an electron-wave Y-branch switch (YBS; Palm and Thylen 1992) where a refractive index change of either branch through an electric field modulation can affect switching. This device, demonstrated in the GaAs/AlGaAs (Worschech et al. 2001) and InP/InGaAs (Hieke and Ulfward 2000, Lewen et al. 2002)-based two-dimensional electron gas (2-DEG) system, relies on ballistic transport and was proposed for low power, ultra-fast (THz) signal processing. It was derived theoretically (Wesstrom 1999) and proven experimentally (Shorubalko et al. 2003) that based on the ballistic electron transport, nonlinear and diode-like *I–V* characteristics were possible. These devices based on III-V materials, while providing proof of concept, were fabricated through conventional lithography. It was also shown in 2-DEG geometry (Song et al. 1998) with artificially constructed defects/barriers, that the defect topology can affect the electron momentum and guide the current to a predetermined spatial location independent of input current direction. This type of rectification involves a new principle of *electron momentum engineering* in contrast to the well-known *band engineering*. Nanotubes provide a more natural avenue to explore such rectification behavior. It was theoretically postulated (Andriotis et al. 2001) that switching and rectification (Figure 10.6) could be observed in symmetric (e.g., no change in chirality from stem to branch) Y-junction SWNTs, assuming quantum conductivity of electrons where the rectification could be determined (Andriotis et al. 2003) by the (1) Formation of a quantum dot/asymmetric scattering center (Song et al. 1998) at the location of the Y-junction (2) Finite length of the stem and branches connected to metallic leads (3) Asymmetry of the bias applied/the potential profile (Tian et al. 1998) across the nanotube (4) Strength of the nanotube–metal lead interactions and influence of the interface (Meunier et al. 2002). Some of the possibilities, where the nature of the individual Y-junction branches determines the electrical transport, are illustrated in Figure 10.7.

10.5 Applications of Y-CNTs to Novel Electronic Functionality

Generally, the motivation for use of new CNT morphologies, such as Y-junctions, based on either SWNTs or MWNTs, in addition to the miniaturization of electronic circuits, is the possible exploration of new devices and technologies through new physical principles. The existence of negative-curvature fullerene-based units (Scuseria 1992), and branching in nanotubes necessitates

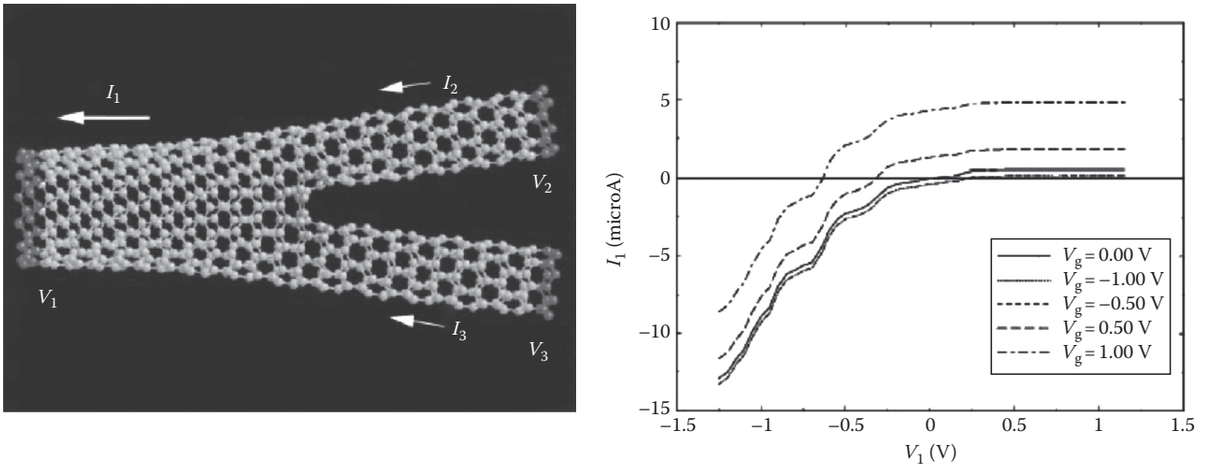

FIGURE 10.6 Asymmetry, and rectification like behavior, in the *I–V* characteristics of a single walled Y-junction nanotube is indicated, through quantum conductivity calculations. (From Andriotis, A.N. et al., *Phys. Rev. Lett.*, 87, 066802, 2001. With permission.)

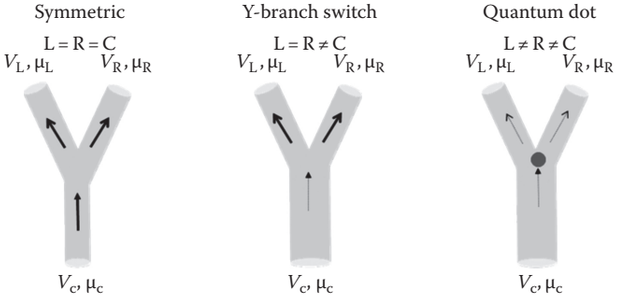

FIGURE 10.7 The CNT Y-junction as a prototypical *structural* element for a variety of functions such as switching or as a quantum dot, depending on the characteristics of the individual branches. L, R, and C, refer to the left, right, and central/stem branches of a Y-junction.

the presence of topological defects—in the form of pentagons, heptagons, and octagons—at the junction regions for maintaining a low energy sp^2 configuration (Andriotis et al. 2002). These *intrinsic* defects are natural scattering centers that could affect/modulate the electrical transport characteristics of a nanotube.

At the nanometer scale, the dimensions of the device are also comparable with the electron wavelength (λ_F) and the electron travel/current must be considered in terms of wave propagation (Davies 1998), analogous to the propagation of light down an optical fiber. Wave phenomena, such as interference and phase shifting, can now be used to construct new types of devices. For example, constructive and destructive interferences can be used to cause transmission and reflection of current leading to switching and transistor-like applications with the added advantage of very low power dissipation. Novel applications have been proposed theoretically (Xu 2001a, 2002b, Csontos and Xu 2003) for ballistic nano-junctions, of which the Y-junction is only one example. Several of these applications have been demonstrated in preliminary experiments and will be elucidated later in the chapter. A brief overview follows.

10.5.1 Switching and Transistor Applications

In a basic Y-junction switch, an electric field can direct electrons into either of two branches, while the other branch is cut off (Wesstrom 1999). It has been shown, in computer simulations (Palm and Thylen 1992), that a sufficient lateral field for electron deflection is created by applying a very small voltage of the order of millivolts (mV). The specific advantage of a Y-junction switch is that it does not need single-mode electron waveguides for its operation and can operate over a wide range of electron velocities and energies, the reason being that the electrons are not stopped by a barrier but are only deflected. An operational advantage over a conventional FET could be that the current is switched between two outputs rather than completely turned on/off (Palm and Thylen 1996), leading to higher efficiency of operation.

An electrical asymmetry can also be induced through structural or chemical means across the two branches in a nanostructured junction. The Y-junction region, for instance, can possess a positive charge (Andriotis et al. 2001) due to two reasons, viz., the presence of (1) topological defects, due to the formation of non-hexagonal polygons at the junction to satisfy the local bond order (Crespi 1998), where delocalization of the electrons over an extended area leads to a net positive charge, and (2) catalyst particles, which are inevitably present during synthesis (Gothard et al. 2004, Teo et al. 2004). This positive charge and the induced asymmetry is analogous to a "gating" action that could be responsible for rectification. While the presence of defects at the junction seems to assist switching, there is also a possibility that such defects may not be needed as some instances of novel switching behavior in Y-junctions are observed in the noticeable absence of catalyst particles. Additional studies are necessary to elucidate this aspect, but such an observation is significant in that a three-dimensional array of Y-junction devices based on CNTs would be much easier to fabricate if a particle is not always required at the junction region.

10.5.2 Rectification and Logic Function

It is possible to design logic circuitry, based on electron wave guiding in Y-junction nanotubes (Xu 2002b), to perform operations similar to and exceeding the performance of conventional electronic devices (Palm and Thylen 1996). When finite voltages are applied to the left and the right branches of a Y-junction, in a push-pull fashion (i.e., $V_{left} = -V_{right}$ or vice versa), the voltage output at the stem would have the same sign as the terminal with the lower voltage. This dependence follows from the principle of continuity of electro-chemical potential ($\mu = -eV$) in electron transport through a Y-junction and forms the basis for the realization of an AND logic gate, i.e., when either of the branch voltages is negative (say, corresponding to a logic state of 0), the voltage at the stem is negative and positive voltage (logic state of 1) at the stem is obtained only when both the branches are at positive biases. The change of μ is also not completely balanced out due to the scattering at the junction, and results in nonlinear interaction of the currents from the left and the right sides (Shorubalko et al. 2003). To compensate, the resultant center branch voltage (V_S) is always negative and varies parabolically (as V^2) with the applied voltage (Xu 2001a).

10.5.3 Harmonic Generation/Frequency Mixing

The nonlinear interaction of the currents and the V^2 dependence of the output voltage at the junction region also suggest the possibility of higher frequency/harmonic generation. When an AC signal of frequency ω, $V_{L-R} = A \cos[\omega t]$, is applied between the left (L) and right (R) branches of the Y-junction, the output signal from the stem (V_S) would be of the form:

$$V_S = \mathbf{a} + \mathbf{b} \cos[2\omega t] + \mathbf{c} \cos[4\omega t]$$

where **a**, **b**, and **c** are constants.

The Y-junction can then be used for second and higher harmonic generation or for frequency mixing (Lewen et al. 2002). The second harmonic (2ω) output is orthogonal to the input voltage and can be easily separated out. These devices can also be used for an ultrasensitive power meter, as the output is linearly proportional to V^2 to very small values of V. A planar CNT Y-junction, with contacts present only at the terminals, suffers from less parasitic effects than a vertical transistor structure and high frequency operation; up to 50 GHz at room temperature (Song et al. 2001), is possible. It can be seen from the brief discussion above that several novel devices can be constructed on CNT Y-junction technology, which could be the forerunner of a new paradigm in nanoelectronics.

10.6 Experimental Work on Electrical Characterization

Compared to the large body of work on electrical transport through linear nanotubes, the characterization of nonlinear nanotubes is still in its infancy. The samples for electrical measurements are typically prepared by suspending nanotube Y-junctions, say, in isopropanol and depositing them on a SiO_2/Si substrate with patterned Au pads. Y-junctions, in proximity to the Au contact pads, are then located at low voltages (<5 kV) using a scanning electron microscope (SEM) and contacts are patterned to each branch of the Y-junction, either through electron-beam lithography (Kim et al. 2006) or focused ion beam induced metal deposition (Gopal et al. 2004), see Figure 10.8. In the latter case, special care needs to be taken not to expose the nanotube to the ion-beam, to prevent radiation damage. The early measurements in Y-junction nanotubes explored the theoretical idea of rectification between any two branches of the Y-junction.

10.6.1 Rectification Characteristics

The initial research in the measurement of the current–voltage (I–V) characteristics of the Y-junctions was accomplished through two-terminal measurements using the stem as one terminal and the two branches, connected together, as the other terminal. With a stem/branch diameter ratio of approximately 60:40 nm, diode-like behavior was observed (Papadapoulos et al. 2000). The authors ascribing SWNT-like p-type semiconductor characteristics, modeled the behavior on a p–p isotype heterojunction where the concentration (N) of carriers (holes) varied inversely as the fourth power of the diameter (D) i.e.,

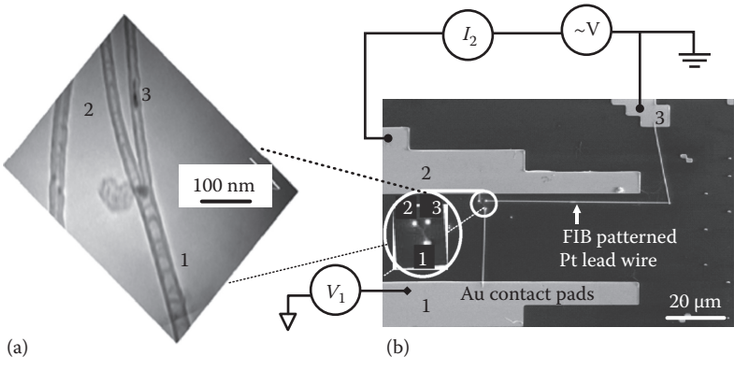

FIGURE 10.8 The (a) MWNT Y-junction electrical measurement configuration as imaged in the (b) SEM.

$N_{\text{stem}}/N_{\text{branch}} \sim \left(D_{\text{branch}}/D_{\text{stem}}\right)^4$. The doping mismatch would then presumably account for the rectifying behavior. In the absence of further characterization, it is difficult to see how semiconducting characteristics could be assigned to >40 nm MWNTs. A subsequent publication from the same group (Perkins et al. 2005) ascribed the electrical characteristics to be dominated by activated conduction, presumably through carrier hopping. More complex nonlinear, quasi-diode-like behavior has been seen (Bandaru et al. 2005) in MWNT Y-junctions (Figure 10.9), which corresponds to a saturation of current at positive bias polarities. This is predicted from theoretical considerations (Xu 2001b) where the current cannot decrease beyond a certain value, but saturates at a value (~0.5 μA at positive V_{1-2}) corresponding to the intrinsic potential of the junction region itself. Such behavior has also been seen in Y-junctions fabricated from 2–DEG systems (Shorubalko et al. 2003, Wallin et al. 2006). The underlying rationale, in more detail, is as follows: the necessity of maintaining a uniform electrochemical potential (μ = eV) in the overall structure gives rise to nonuniform/nonlinear interactions (Xu 2002a). For example, when V_2 (the voltage on branch 2) decreases, μ_2 (= $-eV_2$) increases, and an excess electron current flows towards the central junction. The balance between the *incoming* current and the *outgoing* currents, at the junction itself, is achieved by increasing μ_1 (decreasing V_1). On the other hand, when μ_2 decreases, μ_1 decreases also, but cannot decrease past a certain critical point, viz., the fixed electrochemical potential dictated by the geometry/defects of the junction.

Work on SWNT-based Y-junctions has revealed the diode-like behavior in richer detail. It was established through Raman spectroscopy analyses (Choi and Choi 2005) that constituent Y-junction branches could be either metallic/semiconducting. This gives rise to the possibility of forming intrinsic metal (M)-semiconductor (S) junctions within/at the Y-junction region. Experiments carried out on SWNTs in the 2–5 nm diameter range (Choi and Choi 2005) (which could, depending on the chirality, correspond to either metallic or semiconducting nanotubes with energy gaps in the range of 0.37–0.17 eV (Ding et al. 2002)) reveal ambipolar behavior where carrier transport due to both electrons and holes could be important. Considering, for example, that the Fermi level (E_F) for the metallic branch of the Y-junction is midway through the semiconductor branch band gap, positive or negative biases on the semiconductor branch can induce electron/hole tunneling from the metal (Figure 10.10).

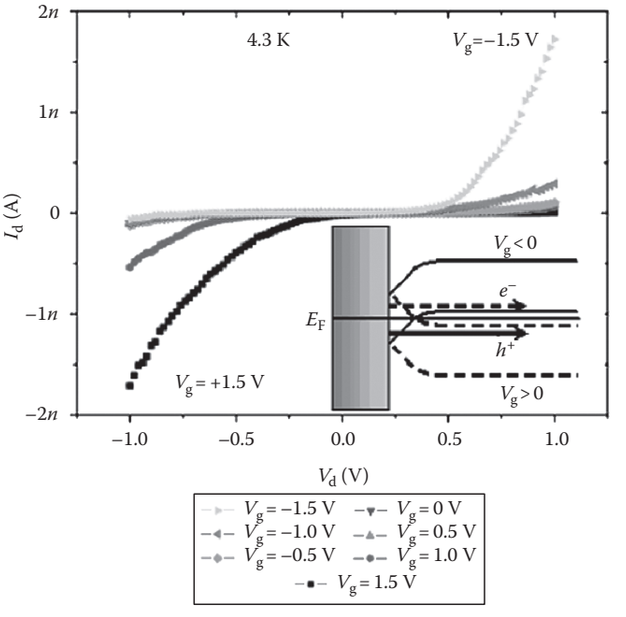

FIGURE 10.10 *I–V* measurements on single walled Y-CNTs, where a metallic CNT interfaces with a semiconducting CNT (see band diagram in inset) indicates ambipolar behavior, as a function of applied gate voltage (on the semiconducting nanotube). (From Kim, D.-H. et al., *Nano Lett.*, 6, 2821, 2006. With permission.)

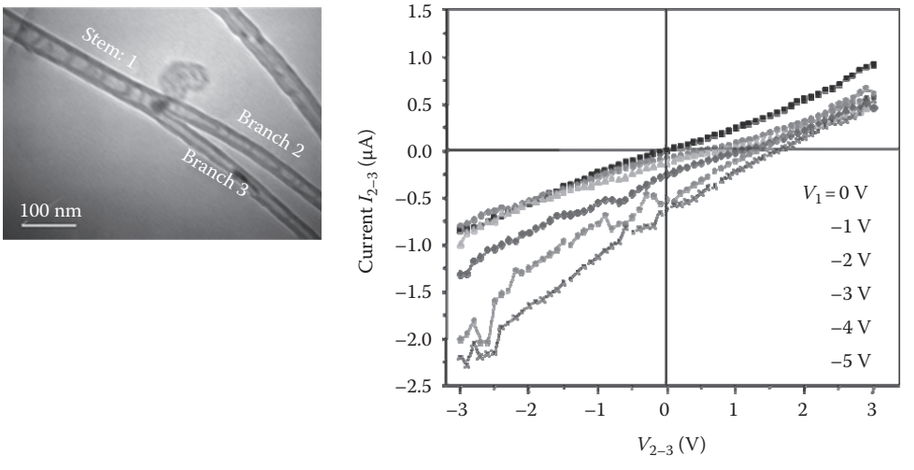

FIGURE 10.9 *I–V* characteristics of a MWNT Y-junction. A constant DC voltage is applied on the stem, while the *I–V* behavior across branches 2 and 3 are monitored. The gating action of the stem voltage (V_1) and the asymmetric response are to be noted.

Such temperature-independent tunneling behavior was invoked through modeling the *I–V* characteristics to be of the Fowler–Nordheim type. However, at higher temperatures (>100 K), thermionic emission corresponding to barrier heights of 0.11 eV could better explain the electrical transport results.

On an interesting note, it should be mentioned that the contact resistance at a branch–metal contact could also play a major role and contribute to the relatively low currents observed in experiments (Meunier et al. 2002). While MWNTs should theoretically have a resistance smaller than h/e^2 (~26 kΩ), ideal and reproducible, Ohmic contacts, through metal evaporation, have been difficult to achieve.

10.6.2 Electrical Switching Behavior

Intriguing experiments have brought forth the possibility of using the CNT Y-junctions for switching applications as an electrical inverter analogous to earlier (Palm and Thylen 1992, Hieke and Ulfward 2000, Shorubalko et al. 2003) Y-switch studies in 2–DEG systems. In this measurement (Bandaru et al. 2005), a DC voltage was applied on one branch of the Y-junction while the current through the other two-branches was probed under a small AC bias voltage (<0.1 V). As the DC bias voltage is increased, at a certain point, the Y-junction goes from nominally conducting to a "pinched-off" state. This switching behavior was observed for all three branches of the Y-junction, at different DC bias voltages. The absolute value of the voltage at which the channel is pinched off is similar for two branches (~2.7 V, as seen in Figure 10.11a and b) and is different for the third stem branch (~5.8 V, as seen in Figure 10.11c). The switching behavior was seen over a wide range of frequencies, up to 50 kHz. The upper limit was set by the capacitive response of the Y-junction when the branch current tends to zero.

The detailed nature of the electrical switching behavior is currently not understood. The presence of catalyst nano-particles (Figure 10.1) in the conduction paths could blockade current flow, and their charging could account for the abrupt drop-off of the current. The exact magnitude of the switching voltage would then be related to the exact size of the nanoparticle, which suggests the possibility of nano-engineering the Y-junction to get a variety of switching behaviors. However, it was deduced (Andriotis and Menon 2006), through tight binding molecular dynamics simulations on SWNTs, that interference effects could be solely responsible for the switching behavior, even in the absence of catalyst particles. An associated possibility is that there is inter-mixing of the currents in the Y-junction, where the

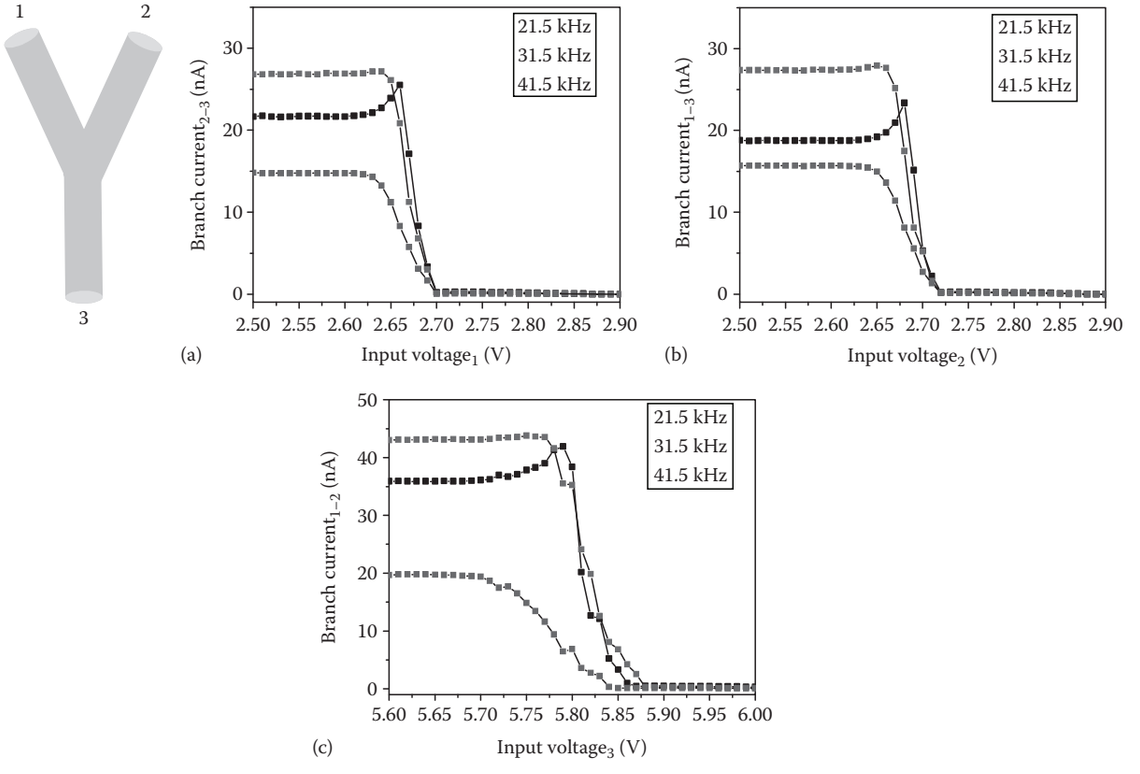

FIGURE 10.11 An abrupt modulation of the current through two branches of the Y-junction, indicative of electrical switching, is seen on varying the voltage on the third branch. The voltage, at which the switching action occurs, on the two branches (1 & 2), is similar and smaller (~2.7 V, see a and b) compared to the turn-off voltage (~5.8 V) on the stem (3) in (c). Such abrupt switching characteristics are seen up to 50 kHz, the upper limit arising from the capacitive response of the Y-junction. (From Bandaru, P.R. et al., *Nature Mater.*, 4, 663, 2005. With permission.)

electron transmission is abruptly cut off due to the compensation of currents, for example, the current through branches 2 and 3 is canceled by current leakage through stem 1. The simultaneous presence of an AC voltage on the source–drain channel and a DC voltage on the control/gate terminal could also result in an abrupt turn-off, due to defect mediated negative capacitance effects (Beale and Mackay 1992). Further research is needed to clarify the exact mechanisms in these interesting phenomena.

A suggestion was also made that AND logic gate behavior could be observed (Bandaru et al. 2005) in a Y-junction geometry. The continuity of the electro-chemical potential from one branch of the CNT Y-junction to another is the basis for this behavior (see Section 10.5.2 for a more detailed explanation).

AQ2

10.6.3 Current Blocking Behavior

Other interesting characteristics were seen when the CNT Y-morphologies were *in situ* annealed in the ambient, in a range of temperatures 20°C–400°C and *I–V* curves measured for various configurations of the Y-junction. The observations are summarized in Figure 10.12 and are fascinating from the point of view of the tunability of electrical characteristics. As the annealing is continued, the onset of nonlinearity in the *I–V* characteristics is observed (Figure 10.12b). With increasing times, the nonlinearity increases, but is *limited* to one polarity of the voltage. This is reminiscent of diode-like behavior and can be modeled as such (Figure 10.12c and inset). With progressive annealing, it was seen that the current is completely cut-off (<1 pA) and perfect rectification seems to be obtained (Figure 10.12d). A current rectification ratio $\left(I_{ON}/I_{OFF}\right)$ of >10^4 has been calculated, where I_{ON} denotes the current through the Y-device at –3 V while I_{OFF} is the current at +3 V. The transition to linear characteristics was more rapid at elevated temperatures of annealing (>200°C). In yet another set of Y-junction samples, reversible behavior from Ohmic to blocking type was observed (Figure 10.13). Interestingly, it was observed that the current through one set of branches (S1–B3 in Figure 10.13b) was not affected by the annealing, while the blocking voltages differ for the other two configurations (viz., ~0.1 V for S1–B2 and ~2.6 V for B2–B3).

The time-dependent behavior and rectification seems to be both a function of temperature and of time of annealing. The sharp cut-off of the current at positive voltages is also remarkable. (The cut-off of the currents at the positive polarity of the voltage seems to be indicative of hole transport in the Y-junctions, through

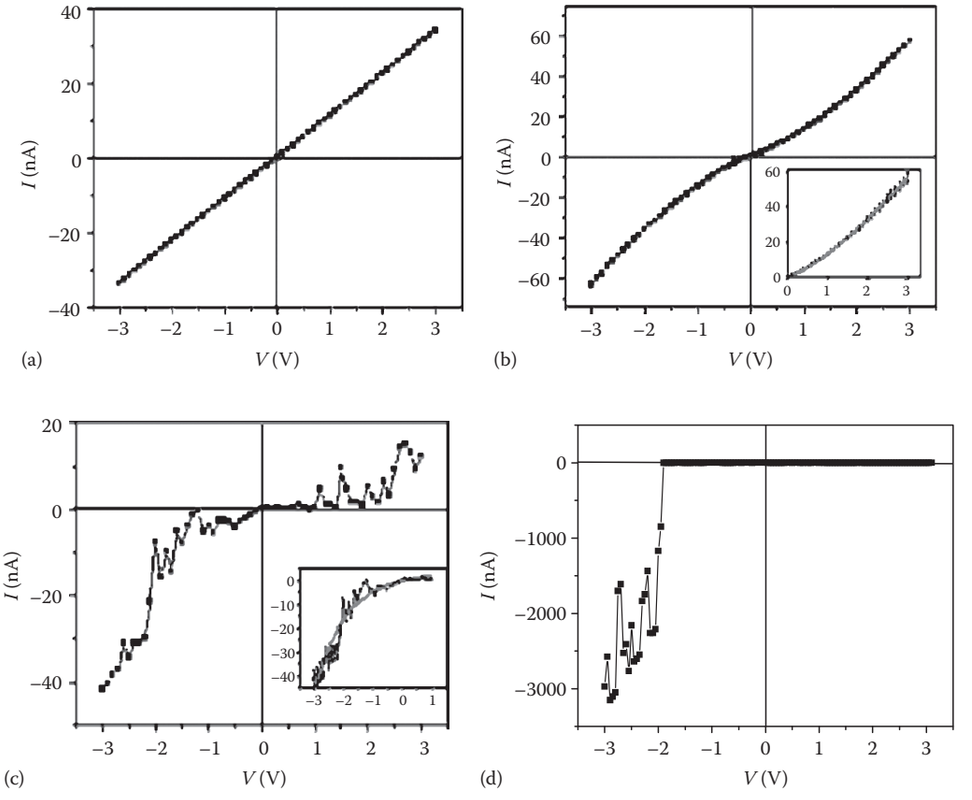

FIGURE 10.12 The *I–V* characteristics for a CNT Y-junction subject to high temperature annealing (~150°C) as a function of annealing time, after being cooled down to room temperature. (a) Prior to annealing Ohmic behavior is observed. At increasing times non-linearity is introduced (b) which can be modeled in terms of space charge currents (see inset) as $I = A\,V + B\,V^{3/2}$. Further annealing results in a (c) diode-like behavior (the inset shows a fit: $I = I_0(e^{(eV/k_BT)} - 1)$ and finally in a (d) current-blocking/rectification behavior where a 10^4 fold suppression in current is seen.

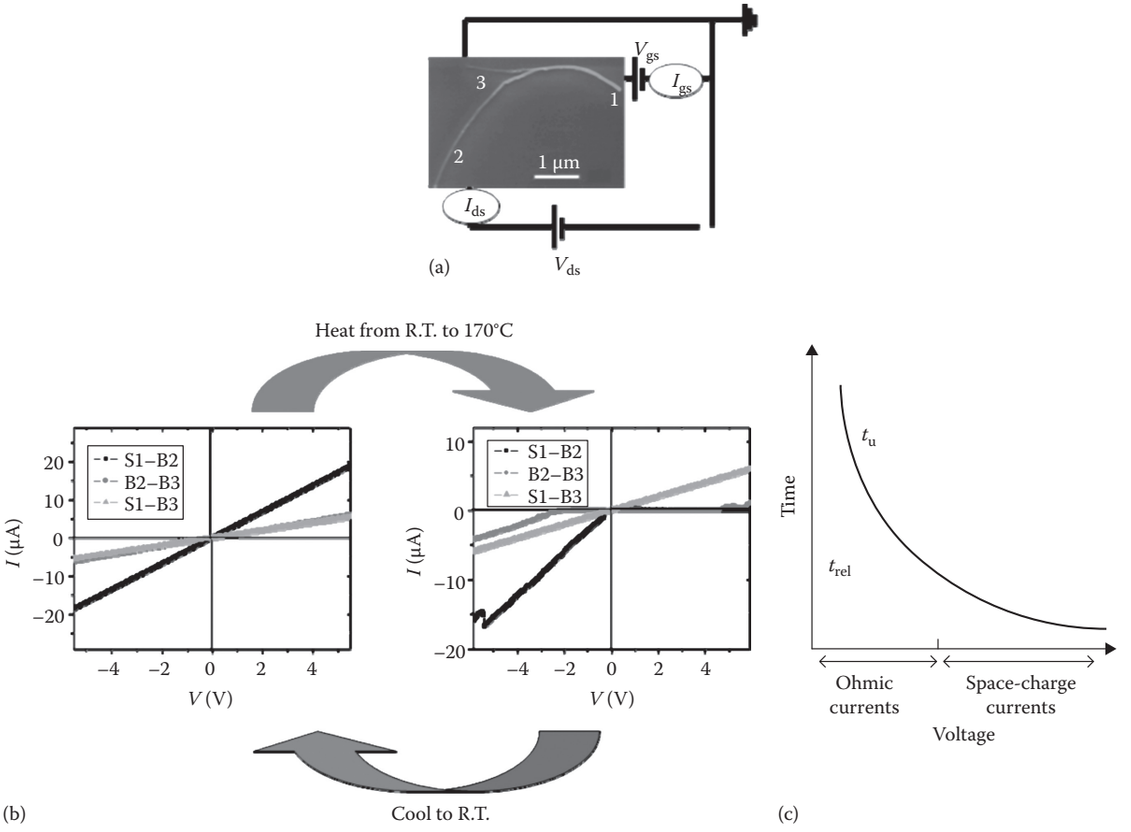

FIGURE 10.13 (a) Circuit arrangement used to probe the *I–V* characteristics of Y-CNT (SEM micrograph). (b) Reversible current blocking behavior induced in the CNT Y-junction. The individual segments' electrical transport characteristics exhibit different blocking/linear characteristics and are geometry dependent. (c) The transition from Ohmic behavior to space charge behavior is a function of voltage and can be accelerated at higher temperatures. The ratio of the transit time (t_{tr}) to the dielectric relaxation time (t_{rel}) determines the dynamics of the carrier transport.

electrostatic doping, due to the work function of Pt, $\phi_{Pt} \sim 5.7$ eV being larger than ϕ_{CNT}.) While it is well known that contacts to p-type CNTs through high work-function metals, where $\phi_M > \phi_{CNT}$ (~4.9 eV) result in Ohmic conduction (Javey et al. 2003, Yang et al. 2005), the transition from conducting to blocking behavior is generally more gradual. A continuous change in the current was also seen when a gate voltage modulates the p-CNT channel conduction and in CNT-based p–n junctions (Lee et al. 2004) with diode-like behavior (Lee et al. 2004, Manohara et al. 2005, Yang et al. 2005). Consequently, we think that the observed behavior is unique to the CNT branched topologies examined here.

The annealing-induced rectification behavior in CNT Y-junctions could be intrinsic to the Y-nanotube form or be related to the nature of the contacts. It was reported that SWNTs contacted by Pt (Javey et al. 2003) could yield nonmetallic behavior, arising from a discontinuous (Zhang et al. 2000) contact layer to the nanotubes. It is also possible that the outer contacting walls of the MWNT Y-junction are affected by the annealing procedure, resulting in a modification of the Schottky barrier (Collins et al. 2001a). Several CNT device characteristics, such as transistors (Appenzeller et al. 2002) and photodetectors (Freitag et al. 2003) are Schottky barrier mediated. Exposure to oxygen is also known to affect the density of states of CNTs and the *I–V* characteristics (Collins et al. 2000). However, the low temperatures (<300°C) employed in the experiment preclude oxidation (Ajayan et al. 1993, Collins et al. 2001b) and the blocking behavior that was observed in our experiment cannot be justified on the above principles.

A hint for explaining this intriguing *I–V* behavior is obtained by modeling the *I–V* characteristics of Figure 10.12b, an intermediate stage in the annealing process. A supra-linear behavior, viz., $\mathbf{I}$ proportional to $A\mathbf{V} + B\mathbf{V}^{3/2}$, can be fitted (Figure 10.12b inset), which could be indicative of space-charge limited currents (A and B are numerical constants). To further understand the transport behavior, it becomes necessary to examine the role of the contacts in detail. Prior to annealing, where we observe linear behavior (Figure 10.12a), i.e., the Ohmic contact is a reservoir of free holes. Generally, the ratio of the hole transit time (t_{tr}) to the dielectric relaxation time (t_{rel}) in the CNT determines the carrier dynamics and currents. A large (t_{tr}/t_{rel}) ratio obtained, say at smaller voltages, would result in Ohmic currents while a lower (t_{tr}/t_{rel}) ratio, at increased voltages, would imply space charge currents (Figure 10.13c). As t_{rel} is inversely proportional (Muller and Kamins 1986) to the conductivity (σ), such effects AQ3

would be more important at elevated temperatures for metallic Y-CNTs. We suggest then that the saturation of the current at positive voltages could be due to space charge effects. In other words, at sufficiently high voltages (>0.1 V for S1–B2 and >2.6 V for B2–B3 in Figure 10.13b), further hole generation is choked due to the preponderance of space charge and negligible current is observed. Note that such a scenario can also be predicted from the band structure diagrams at the metal contact-CNT interface (Figure 10.14). Here, at (ii) forward bias, there is a significant barrier to hole transport and space charge processes could be important. At (iii) negative voltages, however, no hole barriers exist and Ohmic conduction is obtained. The space charge hypothesis is also supported by the observation that over a period of time, the blocking behavior reverts to Ohmic conduction. In an earlier study (Antonov and Johnson 1999) of a straight SWNT diode containing a charged impurity, similar space-charge-based arguments were invoked to explain the observed current rectification. We are currently conducting experiments to probe the time constants and dynamics of current flow through the Y-CNTs.

We speculate that the different diameters of the branches of the Y-junction (Figure 10.1 or Figure 10.13a) could be playing a role in the current blocking behavior. The basis is the observation (Figure 10.13b) where rectification is not observed for a particular (S1–B3) two-terminal configuration. It was found that the magnitude of the conductance ($\mathbf{g_d}$) between any two terminals of the Y-junction is *inversely* proportional to the ratio of the diameters through which the current is flowing (see Figure 10.13b), i.e., a larger discrepancy between the branch diameters lowers the conductance. In an analogy to fluid flow through a pipe, the hole current can similarly be modulated by the Y-junction geometry. It would be instructive to characterize the blocking behavior systematically as a function of branch diameters in the Y-junction geometry.

The phenomena of current being low when the voltage was high, in terms of space charge distribution was noted by Shockley (1950), who remarked on its presence in the collector region of a junction transistor amplifier. The *I–V* characteristics observed in the CNT Y-junction forms here could be compared to that of a transit-time device such as a barrier injection and transit time (BARITT) diode (Streetman and Banerjee 2000). Such devices consider space charge limited currents for creating *negative resistance* regions, which can be exploited for switching, oscillation, amplification, and other functions in

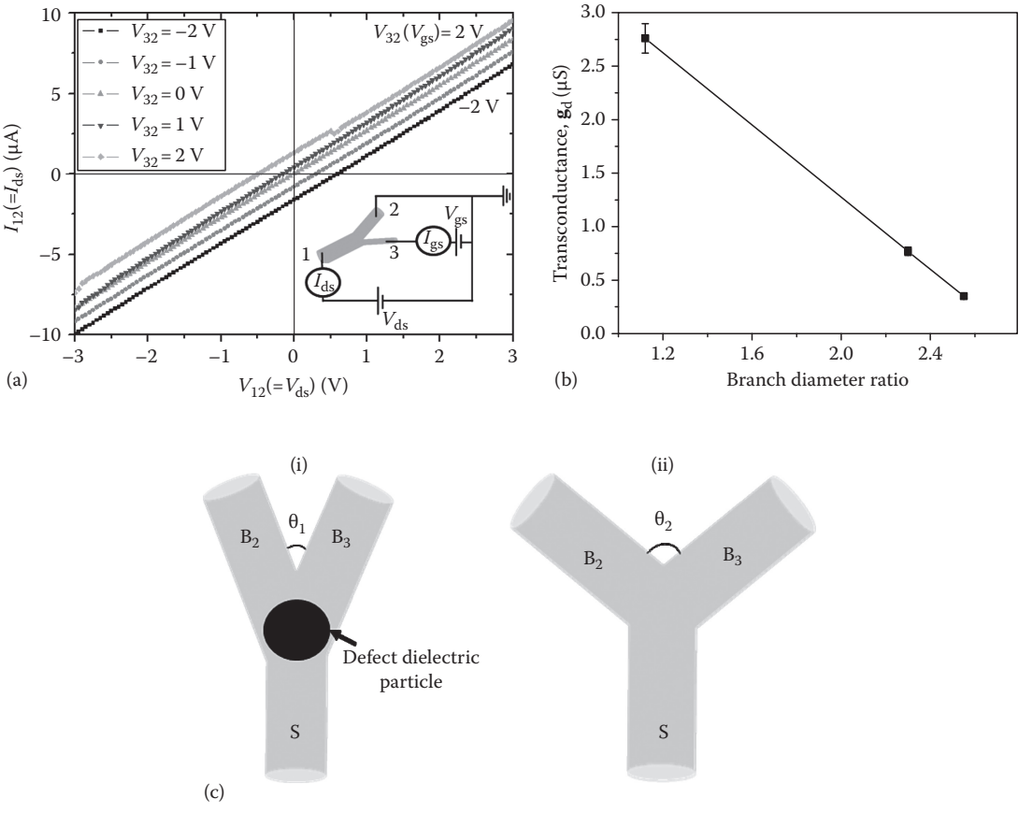

FIGURE 10.14 (a) *I–V* characteristics of a Y-CNT consisting of metallic branches. The circuit diagram is indicated in the inset. (b) The conductance ($\mathbf{g}_d$) through two nanotubes of different diameters in the Y-CNT is inversely proportional to their ratio (= $d_>/d_<$). (c) Proposed Y-junction CNT based switching devices, (i) where a smaller angle (θ_1) between the branches (B_2 and B_3) can result in a higher gating efficiency for the stem (S). (ii) A Y-CNT with uniform gating/electrical switching characteristics can be fabricated by synthesizing all the constituent nanotubes to be of the same diameter and with $\theta_2 = 120°$. (From Park, J. et al., *Appl. Phys. Lett.*, 88, 243113, 2006. With permission.)

high-speed circuitry (Sze 1981). The time delay associated with space charge dissipation is useful for generating microwaves and the BARITT devices are consequently used as local oscillators in microwave receivers.

10.6.4 Metallic Y-Junctions

It is also possible that the constituent nanotubes in the Y-junction can exhibit metallic conduction, in which case the behavior is analogous to that of three interconnected metal lines! Such behavior has indeed been observed (Park et al. 2006) (Figure 10.14a). A control voltage (V) is applied on one of the three terminals (gate) of the Y-CNT while the current (I) through the other two terminals (source and drain) is monitored. The I–V curves of the Y-CNTs, as a function of gate (V_{gs})/bias (V_{ds}) voltage, are shown in Figure 10.14a. The notable features are: (a) Ohmic conduction, (b) a proportional displacement of the current with V_{gs} and V_{ds}, and (c) a geometry dependent conductance. The devices are also seen to have both current and voltage gain. In line with an earlier study (Perkins et al. 2005), we define the differential current gain ($\mathbf{g_{diff}}$) as the ratio of $\left(\partial I_{gs}/\partial V_{gs}\right)$ to $\left(\partial I_{ds}/\partial V_{gs}\right)$ at a constant source–drain voltage (V_{ds}). In our Y-CNT devices, a $\mathbf{g_{diff}}$ of up to 10 is obtained at room temperature. The voltage gain is calculated (Tans et al. 1998) by considering the voltage change (ΔV_{ds}) for a given increment in gate voltage (ΔV_g), at a constant value of the current. The voltage gain when the stem (1 in Figure 10.13a) is used for electrical gating is ~6 while the value drops to ~0.3 when the branch (3 in Figure 10.13a) is used for a gate.

Other quantities of importance in quantifying the electrical characteristics are the *transconductance*, $\mathbf{g_m} = \left(\partial I_{ds}/\partial V_{gs}\right)_{V_{ds}}$, the ratio of the output current (I_{ds}) to the modulating/gating voltage (V_{gs}) at a constant bias voltage (V_{ds}), and the *output conductance*, $\mathbf{g_d} = \left(\partial I_{ds}/\partial V_{ds}\right)_{V_{gs}}$, the ratio of the output current to the bias voltage at a constant gate voltage. It was found that the magnitude of the $\mathbf{g_d}$ is *inversely* proportional to the ratio of the diameters of the branches through which the current is flowing (Figure 10.14b), i.e., a larger discrepancy between the branch diameters lowers the conductance. On the other hand, the $\mathbf{g_m}$, which denotes the gating efficiency for current modulation, seems to be *directly* proportional to the diameter of the gating nanotube (Park et al. 2006).

From the Y-CNT electrical characteristics, it is seen that the mode of operation of the device is quite different from that of a conventional FET and more akin to a Schottky barrier type FET (Muller and Kamins 1986). The current modulation is controlled by the electric field ($= \nabla_{\mathbf{r}} . \mathbf{V}$) at the gating terminal, and not the carrier density in the channel. In this case, the device performance can be improved by increasing the diameter of the gate so as to have a greater modulating effect on the source–drain current. The assumption of electric field control can also be tested (Park et al. 2006) by varying the angle (θ) between the branches of the Y-CNT. From elementary electrostatics (Jackson 1999), the surface-charge density at a distance, ρ, from the intersection of the gate with the junction varies as $\rho^{(\pi/\theta-1)}$, which implies a greater modulating effect at a sharper angle. As an example, for the Y-CNT in Figure 10.4a, the stem would have a higher gating efficiency than in case (b). The manipulation of the junction region to be dielectric/insulating (say, by localized ion-implantation) can also be used to change the electrochemical potential and vary device characteristics. It is interesting to note the similarity of Figure 10.14c to a Metal Oxide Semiconductor Field Effect Transistor (MOSFET), where the stem is analogous to a *gate*, the dielectric particle plays the role of the *gate oxide*, and the *channel* is formed by conduction through the branches. On the other hand, uniform electrical gating/switching characteristics could be obtained by making all the nanotubes the same diameter and length, at an angle of 120° to each other (Figure 10.14c(ii)).

We also suggest that even more interesting applications are facilitated by our experimental results and observations. For example, a single Y-CNT switching device can be made to have diverse operating characteristics through the use of different gating terminals. Technology based on Y-junctions can be used for devices (1) with multiple programmable characteristics and (2) as components in Field Programmable Gate Arrays (FPGAs) for reconfigurable computing (Rabaey 1996), where it would be possible to dynamically alter circuit paths. The large scale integration density and high speed of signal propagation intrinsic to nanotubes would be advantageous in this regard.

10.7 Topics for Further Investigation

For the novel applications of Y-CNTs to be practicable, it would be important and necessary to gain better control of the geometry, through synthesis or processing, of Y-CNTs. It is plausible that the remarkable features of Y-junction-based transistors such as the abrupt switching (Bandaru et al. 2005) and differential gain (Perkins et al. 2005) observed in earlier studies could be related to the presence and location of defects. *In situ* engineering of CNT morphology, e.g., exposure to intense electron-beam radiation (Terrones et al. 2002) could also be utilized to tailor individual Y-CNT characteristics. Other aspects that merit further study include the following:

a. The characterization of the detailed morphology of the Y-junctions and their effect on the electrical properties. Catalyst particles have been found both at the junction, along the length of the Y-junctions and at the tips (Li et al. 2001) (Figure 10.1). The effect of the location, type, and composition of these particles and their scattering characteristics on the electrical transport would yield insight into their influence.
b. A detailed study of the growth mechanisms of multi-junction carbon nanotubes vis-à-vis the influence of the catalyst particles. It has been contended (Teo et al. 2004) that a perturbation during growth could promote

the formation of branches/junctions. For example, if the temperature is reduced during the growth process, a catalyst particle over-saturated with carbon can be induced to nucleate another branch. On the other hand, if the Ti catalyst does play a role, the importance of carbide formers in inducing side-branch growth is interesting from a basic thermodynamic point of view, i.e., is a high negative heat of formation (ΔH_f) of the carbide formers necessary? It is worth noting that Y-junctions and other morphologies, such as H-junctions and T-junctions (Ting and Chang 2002), are also formed when methane (which could yield positive ΔH_f) is used as a precursor. The composition of the catalyst particle, which nucleates the nanotube branches (Teo et al. 2004), and the effects of stress generated at the growing nanotube tips could also be playing important roles (Ting and Chang 2002) in Y-junction growth.

c. The issue of electrical conductivity through nanotubes with bends, junctions, and catalyst particles, which is also important for the future viability of nanotube-based electronics. While the MWNT has an intrinsic resistance, say due to ballistic transport, a capacitive and inductive component will also have to be considered due to the presence of particles, inter-tube transport etc. Such a study will also yield insight into the speed of operation of the nanotube-based devices and affecting factors, in terms of the RC delay. It has been theoretically proposed (Burke 2003) that *straight* SWNTs are capable of THz operation and can even be used as nano-antennae (Burke 2002) for radiation and detection in these very high frequency ranges. Whether SWNT or MWNT Y-junctions are capable of being operated at such high frequencies, due to the presence of defects, and determining an ultimate limit (Guo et al. 2002) to their performance is worth investigating.

d. It has been proposed (Xu 2005), that novel CNT-based circuits based on Y-junctions and branched morphologies can be created. These circuits could be fabricated so as to construct universal logic gates such as NAND/X-NOR. Such a demonstration together with the possibility of multifunctionality, e.g., where the catalyst particle could be used for photon detection (Kosaka et al. 2002) will be important. A variety of such novel circuits can be fabricated leading to a potentially new paradigm for nanoelectronics that goes well beyond traditional FET architectures-shape controlled logic elements.

e. Assembly into a viable circuit topology and large scale fabrication are issues that are of paramount importance. Currently, the Y-junctions are grown in mats/bundles and individually isolated and measured. A scheme where each junction is assembled in this way is not viable practically. Ideas into self-assembly and controlled placement (Huang et al. 2005) of nanotubes will have to be addressed. While some measure of success has been achieved in coordinating the placement of loose nanotubes, e.g., through the use of chemically functionalized substrates (Liu et al. 1999) along with dip-pen lithography (Rao et al. 2003), an orienting electric field-exploiting the nanotubes' dipole character (Joselevich and Lieber 2002), through magnetic field (Hone et al. 2000), and microfluidic arrangements (Huang et al. 2001), assembly of such loose nanotubes is difficult to scale up and still remains a critical issue. An array of Y-junctions can be prepared on the same nanotube stem, as was found in preliminary studies, by exposing only periodic locations (Qin et al. 2005) along the length of a nanotube, sputter depositing catalyst, and growing parallel Y-junction branches from this linear array of catalysts using electric field-induced direction control during a subsequent CVD process, e.g., at any angle from the main stem. The above growth technique could be used to make multiple Y-junction devices in series/parallel. This proof of growth will go a long way in demonstrating the feasibility of large scale nanoelectronic device assembly—a question of the highest importance in recent times.

AQ5

10.8 Conclusions

The study of Y-junctions is still in its infancy. Their synthesis, while reasonably reproducible, is still challenging in terms of the precise placement on a large scale. It is worth mentioning that this is an issue even with linear nanotubes and might well determine the feasibility of CNT applications, in general. Presently, both single-walled and multi-walled Y-CNTs, the constituent branches of which could have different diameters or semiconducting/metallic character, have been synthesized. Such internal diversity gives rise to novel phenomena such as (1) rectification/current blocking behavior, (2) electrical switching, and (3) logic gate characteristics. It is also interesting to investigate whether the three terminals of the Y-CNT can be interfaced into a transistor-like paradigm. Future investigations should correlate the detailed physical structure of the nanostructure morphologies with the electrical measurements to gain a better understanding of the conduction processes vis-à-vis the role of defects and geometry in nonlinear structures. Such a comprehensive and correlated study would be useful to the nanotube/nanowire community and could pave the way to the realization of *shape controlled* nanoelectronic devices exclusive to the nanoscale.

References

Ajayan, P.M., 1999. Nanotubes from carbon. *Chemical Reviews*, 99, 1787–1799.

Ajayan, P.M., Ebbesen, T.W., Ichihashi, T. et al., 1993. Opening carbon nanotubes with oxygen and implications for filling. *Nature*, 362, 522–525.

Andriotis, A.N. and Menon, M., 2006. Are electrical switching and rectification inherent properties of carbon nanotube Y-junctions? *Applied Physics Letters*, 89, 132116.

Andriotis, A.N., Menon, M., Srivastava, D. et al., 2001. Rectification properties of carbon nanotube "Y-junctions". *Physical Review Letters*, 87(6), 066802.

Andriotis, A.N., Menon, M., Srivastava, D. et al., 2002. Transport properties of single-wall carbon nanotube Y-junctions. *Physical Review B*, 65, 165416.

Andriotis, A.N., Srivastava, D., and Menon, M., 2003. Comment on Intrinsic electron transport properties of carbon nanotube Y-junctions. *Applied Physics Letters*, 83, 1674–1675.

Antonov, R.D. and Johnson, A.T., 1999. Subband population in a single-wall carbon nanotube diode. *Physical Review Letters*, 83, 3274–3276.

Appenzeller, J., Knoch, J., Martel, R. et al., 2002. Carbon nanotube electronics. *IEEE Transactions on Nanotechnology*, 1, 184–189.

Bachtold, A., Hadley, P., Nakanishi, T. et al., 2001. Logic circuits with carbon nanotube transistors. *Science*, 294, 1317–1320.

Bachtold, A., Strunk, C., Salvetat, J.-P. et al., 1999. Aharonov-Bohm oscillations in carbon nanotubes. *Nature*, 397, 673–675.

Bandaru, P.R., 2007. Electrical properties and applications of carbon nanotube structures. *Journal of Nanoscience and Nanotechnology*, 7, 1239–1267.

Bandaru, P.R., Daraio, C., Jin, S. et al., 2005. Novel electrical switching behavior and logic in carbon nanotube Y-junctions. *Nature Materials*, 4, 663–666.

Bandaru, P.R., Daraio, C., Yang, K. et al., 2007. A plausible mechanism for the evolution of helical forms in nanostructure growth. *Journal of Applied Physics*, 101, 094307.

Baughman, R.H., Zakhidov, A.A., and De Heer, W.A., 2002. Carbon nanotubes-the route toward applications. *Science*, 297, 787.

Beale, M. and Mackay, P., 1992. The origins and characteristics of negative capacitance in metal-insulator-metal devices. *Philosophical Magazine B*, 65, 47–64.

Bockrath, M., Cobden, D.H., Mceuen, P.L. et al., 1997. Single-electron transport in ropes of carbon nanotubes. *Science*, 275, 1922–1924.

Buitelaar, M.R., Bachtold, A., Nussbaumer, T. et al., 2002. Multiwall carbon nanotubes as quantum dots. *Physical Review Letters*, 88, 156801.

Burke, P.J., 2002. Luttinger liquid theory as a model of the gigahertz electrical properties of carbon nanotubes. *IEEE Transactions on Nanotechnology*, 1, 129–144.

Burke, P.J., 2003. An RF circuit model for carbon nanotubes. *IEEE Transactions on Nanotechnology*, 2(1), 55–58.

Castrucci, P., Scarselli, M., De Crescenzi, M. et al., 2004. Effect of coiling on the electronic properties along single-wall carbon nanotubes. *Applied Physics Letters*, 85, 3857–3859.

Choi, Y.C. and Choi, W., 2005. Synthesis of Y-junction single-wall carbon nanotubes. *Carbon*, 43, 2737–2741.

Collins, P.G., Arnold, M.S., and Avouris, P., 2001a. Engineering carbon nanotubes and nanotube circuits using electrical breakdown. *Science*, 292, 706–709.

Collins, P.G. and Avouris, P., 2000. Nanotubes for electronics. *Scientific American*, December, 62–69.

Collins, P.G., Bradley, K., Ishigami, M. et al., 2000. Extreme oxygen sensitivity of electronic properties of carbon nanotubes. *Science*, 287, 180–1804.

Collins, P.G., Hersam, M., Arnold, M. et al., 2001b. Current saturation and electrical breakdown in mutiwalled carbon nanotubes. *Physical Review Letters*, 86, 3128–3131.

Crespi, V.H., 1998. Relations between global and local topology in multiple nanotube junctions. *Physical Review B*, 58, 12671.

Csontos, D. and Xu, H.Q., 2003. Quantum effects in the transport properties of nanoelectronic three-terminal Y-junction devices. *Physical Review B*, 67, 235322.

Dai, H., 2001. Nanotube growth and characterization. In Dresselhaus, M.S., Dresselhaus, G., and Avouris, P. eds., *Topics in Applied Physics*. Berlin: Springer-Verlag, pp. 29–53.

Dai, H., 2002. Carbon nanotubes: From synthesis to integration and properties. *Accounts of Chemical Research*, 35, 1035–1044.

Davies, J.H., 1998. *The Physics of Low-Dimensional Semiconductors*. New York: Cambridge University Press.

Delaney, P., Di Ventra, M., and Pantelides, S., 1999. Quantized conductance of multiwalled carbon nanotubes. *Applied Physics Letters*, 75, 3787–3789.

Ding, J.W., Yan, X.H., and Cao, J.X., 2002. Analytical relation of band gaps to both chirality and diameter of single-wall carbon nanotubes. *Physical Review B: Condensed Matter*, 66, 073401.

Dresselhaus, M.S., Dresselhaus, G., and Jorio, A., 2004. Unusual properties and structure of carbon nanotubes. *Annual Review of Materials Research*, 34, 247–278.

Forro, L. and Schonenberger, C., 2001. Physical properties of multi-wall nanotubes. In Dresselhaus, M.S., Dresselhaus, G., and Avouris, P. eds., *Carbon Nanotubes—Topics in Applied Physics*. Heidelberg: Springer-Verlag.

Freitag, M., Martin, Y., Misewich, J.A. et al., 2003. Photoconductivity of single carbon nanotubes. *Nano Letters*, 3, 1067–1071.

Freitag, M., Radosavljevic, M., Zhou, Y. et al., 2001. Controlled creation of a carbon nanotube diode by a scanned gate. *Applied Physics Letters*, 79, 3326–3328.

Fuhrer, M.S., Nygard, J., Shih, L. et al., 2000. Crossed nanotube junctions. *Science*, 288, 494.

Gopal, V., Radmilovic, V.R., Daraio, C. et al., 2004. Rapid prototyping of site-specific nanocontacts by electron and ion beam assisted direct-write nanolithography. *Nano Letters*, 4, 2059–2063.

Gothard, N., Daraio, C., Gaillard, J. et al., 2004. Controlled growth of Y-junction nanotubes using ti-doped vapor catalyst. *Nano Letters*, 4(2), 213–217.

Guo, J., Datta, S., Lundstrom, M. et al., 2002. Assessment of silicon mos and carbon nanotube fet performance limits using a general theory of ballistic transistors. *International Electron Devices Meeting* (*IEDM*), San Francisco, CA, pp. 711–714.

Hieke, K. and Ulfward, M., 2000. Nonlinear operation of the Y-branch switch: Ballistic switching mode at room temperature. *Physical Review B*, 62, 16727–16730.

Hone, J., Laguno, M.C., Nemes, N.M. et al., 2000. Electrical and thermal transport properties of magnetically aligned single wall carbon nanotube films. *Applied Physics Letters*, 77, 666.

Huang, X.M.H., Caldwell, R., Huang, L. et al., 2005. Controlled placement of individual carbon nanotubes. *Nano Letters*, 5, 1515–1518.

Huang, Y., Duan, X., Wei, Q. et al., 2001. Directed assembly of one-dimensional nanostructures into functional networks. *Science*, 291, 630–633.

Iijima, S., Ichihashi, T., and Ando, Y., 1992. Pentagons, heptagons and negative curvature in graphite microtubule growth. *Nature*, 356, 776–778.

Jackson, J.D., 1999. *Classical Electrodynamics*. New York: John Wiley & Sons.

Javey, A., Guo, J., Wang, Q. et al., 2003. Ballistic carbon nanotube field-effect transistors. *Nature*, 424, 654–657.

Joselevich, E. and Lieber, C.M., 2002. Vectorial growth of metallic and semiconducting single-wall carbon nanotubes. *Nano Letters*, 2, 1137–1141.

Kang, S.J., Kocabas, C., Ozel, T. et al., 2007. High-performance electronics using dense, perfectly aligned arrays of single-walled carbon nanotubes. *Nature Nanotechnology*, 2, 230–236.

Kim, D.-H., Huang, J., Shin, H.-K. et al., 2006. Transport phenomena and conduction mechanisms of single walled carbon nanotubes (SWNTs) at Y- and crossed junctions. *Nano Letters*, 6, 2821–2825.

Kim, P., Shi, L., Majumdar, A. et al., 2001. Thermal transport measurements of individual multiwalled nanotubes. *Physical Review Letters*, 87, 215502.

Kosaka, H., Rao, D.S., Robinson, H. et al., 2002. Photoconductance quantization in a single-photon detector. *Physical Review B (Rapid Communications)*, 65, 201307.

Lee, J.U., Gipp, P.P., and Heller, C.M., 2004. Carbon nanotube p-n junction diodes. *Applied Physics Letters*, 85, 145–147.

Lewen, R., Maximov, I., Shorubalko, I. et al., 2002. High frequency characterization of gainas/inp electronic waveguide tbs switch. *Journal of Applied Physics*, 91, 2398–2402.

Li, W.Z., Wen, J.G., and Ren, Z.F., 2001. Straight carbon nanotube y junctions. *Applied Physics Letters*, 79, 1879–1881.

Liu, J., Casavant, M.J., Cox, M. et al., 1999. Controlled deposition of individual single-walled carbon nanotubes on chemically functionalized templates. *Chemical Physics Letters*, 303, 125–129.

Manohara, H.M., Wong, E.W., Schlecht, E. et al., 2005. Carbon nanotube Schottky diodes using ti-schottky and pt-ohmic contacts for high frequency applications. *Nano Letters*, 5, 1469–1474.

Martel, R., Derycke, V., Appenzeller, J. et al., 2002. Carbon nanotube field-effect transistors and logic circuits. *Design Automation Conference, ACM*, New Orleans, LA.

Mceuen, P.L., 1998. Carbon-based electronics. *Nature*, 393, 15–16.

Mceuen, P.L., Fuhrer, M.S., and Park, H., 2002. Single-walled carbon nanotube electronics. *IEEE Transactions on Nanotechnology*, 1, 78–85.

Meunier, V., Nardelli, M.B., Bernholc, J. et al., 2002. Intrinsic electron transport properties of carbon nanotube Y-junctions. *Applied Physics Letters*, 81, 5234–5236.

Muller, R.S. and Kamins, T.I., 1986. *Device Electronics for Integrated Circuits,* 2nd edn. New York: John Wiley & Sons.

Nichols, J.A., Saito, H., Deck, C. et al., 2007. Artificial introduction of defects into vertically aligned multiwall carbon nanotube ensembles: Application to electrochemical sensors. *Journal of Applied Physics*, 102, 064306.

Palm, T. and Thylen, L., 1992. Analysis of an electron-wave Y-branch switch. *Applied Physics Letters*, 60, 237–239.

Palm, T. and Thylen, L., 1996. Designing logic functions using an electron waveguide Y-branch switch. *Journal of Applied Physics*, 79, 8076–8081.

Papadapoulos, C., Rakitin, A., Li, J. et al., 2000. Electronic transport in Y-junction carbon nanotubes. *Physical Review Letters*, 85, 3476–3479.

Park, J., Daraio, C., Jin, S. et al., 2006. Three-way electrical gating characteristics of metallic Y-junction carbon nanotubes. *Applied Physics Letters*, 88, 243113.

Perkins, B.R., Wang, D.P., Soltman, D. et al., 2005. Differential current amplification in three-terminal Y-junction carbon nanotube devices. *Applied Physics Letters*, 87, 123504.

Postma, H.W.C., Teepen, T., Yao, Z. et al., 2001. Carbon nanotube single-electron transistors at room temperature. *Science*, 293, 76–79.

Qin, L., Park, S., Huang, L. et al., 2005. On-wire lithography. *Science*, 309, 113–115.

Rabaey, J., 1996. *Digital Integrated Circuits: A Design Perspective*. New York: Prentice Hall.

Radosavljevic, M., Freitag, M., Thadani, K.V. et al., 2002. Non- AQ6
volatile molecular memory elements based on ambipolar nanotube field effect transistors. *Nano Letters*, 2(7), 761–764.

Rao, S.G., Huang, L., Setyawan, W. et al., 2003. Large-scale assembly of carbon nanotubes. *Nature*, 425, 36–37.

Rueckes, T., Kim, K., Joselevich, E. et al., 2000. Carbon nanotube-based nonvolatile random access memory for molecular computing. *Science*, 289, 94–97.

Saito, R., Dresselhaus, G., and Dresselhaus, M.S., 1998. *Physical Properties of Carbon Nanotubes*. London: Imperial College Press.

Satishkumar, B.C., Thomas, P.J., Govindaraj, A. et al., 2000. Y-junction carbon nanotubes. *Applied Physics Letters*, 77, 2530–2532.

Scuseria, G.E., 1992. Negative curvature and hyperfullerenes. *Chemical Physics Letters*, 195, 534–536.

Shockley, W., 1950. *Electrons and Holes in Semiconductors*. New York: D. Van. Nostrand Company.

Shorubalko, I., Xu, H.Q., Omling, P. et al., 2003. Tunable nonlinear current-voltage characteristics of three-terminal ballistic nanojunctions. *Applied Physics Letters*, 83, 2369–2371.

Song, A.M., Lorke, A., Kriele, A. et al., 1998. Nonlinear electron transport in an asymmetric microjunction: A ballistic rectifier. *Physical Review Letters*, 80, 3831–3834.

Song, A.M., Omling, P., Samuelson, L. et al., 2001. Room-temperature and 50 GHz operation of a functional nanomaterial. *Applied Physics Letters*, 79, 1357–1359.

Streetman, B.G. and Banerjee, S., 2000. *Solid State Electronic Devices*, 5th edn., Upper Saddle River, NJ: Prentice Hall.

Sze, S.M., 1981. *Physics of Semiconductor Devices*, 2nd edn. New York: John Wiley & Sons.

Tans, S.J., Devoret, M.H., Dai, H. et al., 1997. Individual single-wall carbon nanotubes as quantum wires. *Nature*, 386, 474–477.

Tans, S.J., Verschueren, A.R.M., and Dekker, C., 1998. Room-temperature transistor based on a single carbon nanotube. *Nature*, 393, 49–52.

Teo, K.B.K., Singh, C., Chhowalla, M. et al., 2004. Catalytic synthesis of carbon nanotubes and nanofibers. In Nalwa, H.S. ed., *Encyclopedia of Nanoscience and Nanotechnology*. Stevenson Ranch, CA: American Scientific Publishers.

Terrones, M., Banhart, F., Grobert, N. et al., 2002. Molecular junctions by joining single-walled carbon nanotubes. *Physical Review Letters*, 89, 075505.

Tian, W., Datta, S., Hong, S. et al., 1998. Conductance spectra of molecular wires. *Journal of Chemical Physics*, 109, 2874–2882.

Ting, J.-M. and Chang, C.-C., 2002. Multijunction carbon nanotube network. *Applied Physics Letters*, 80, 324–325.

Tsukagoshi, K., Watanabe, E., Yagi, I. et al., 2004. Multiple-layer conduction and scattering property in multi-walled carbon nanotubes. *New Journal of Physics*, 6, 1–13.

AQ7 Wallin, D., Shorubalko, I., Xu, H.Q. et al., 2006. Nonlinear electrical properties of three-terminal junctions. *Applied Physics Letters* (to be published).

Wesstrom, J.O., 1999. Self-gating effect in the electron Y-branch switch. *Physical Review Letters*, 82, 2564–2567.

White, C.T. and Todorov, T.N., 1998. Carbon nanotubes as long ballistic conductors. *Nature*, 393, 240.

Worschech, L., Xu, H.Q., Forchel, A. et al., 2001. Bias-voltage-induced asymmetry in nanoelectronic y-branches. *Applied Physics Letters*, 79, 3287–3289.

Xu, H.Q., 2001a. Diode and transistor behaviors of three-terminal ballistic junctions. *Applied Physics Letters*, 80, 853–855.

Xu, H.Q., 2001b. Electrical properties of three-terminal ballistic junctions. *Applied Physics Letters*, 78(14), 2064–2066.

Xu, H.Q., 2002a. Diode and transistor behaviors of three-terminal ballistic junctions. *Applied Physics Letters*, 80, 853–855.

Xu, H.Q., 2002b. A novel electrical property of three-terminal ballistic junctions and its applications in nanoelectronics. *Physica E*, 13, 942–945.

Xu, H.Q., 2005. The logical choice for electronics? *Nature Materials*, 4, 649–650.

Yang, M.H., Teo, K.B.K., Milne, W.I. et al., 2005. Carbon nanotube schottky diode and directionally dependent field-effect transistor using asymmetrical contacts. *Applied Physics Letters*, 87, 253116.

Yao, Z., Postma, H.W.C., Balents, L. et al., 1999. Carbon nanotube intramolecular junctions. *Nature*, 402, 273–276.

Zhang, Y., Franklin, N.W., Chen, R.J. et al., 2000. Metal coating on suspended carbon nanotubes and its implication to metal-tube interaction. *Chemical Physics Letters*, 331, 35–41.

Zhou, D. and Seraphin, S., 1995. Complex branching phenomena in the growth of carbon nanotubes. *Chemical Physics Letters*, 238, 286–289.

Author Queries

[AQ1] Please review the sentence beginning with "Nanotube junctions were…" for sense.
[AQ2] Please check the updated section number.
[AQ3] Please review the sentence beginning with "Prior to annealing …" for clarity.
[AQ4] Please review the sentence beginning with "The I–V characteristics…" for clarity.
[AQ5] Please review the sentence beginning with "While some measure…" for clarity.
[AQ6] Please check the inserted information for Radosavljevic, 2002.
[AQ7] Please update Wallin et al. 2006.